COMPUTATIONAL MECHANICS 2021
36th conference with international participation
Srní
November 8 - 10, 2021

In vitro structured tree model of the peripheral vascular network

J. Kohút, J. Jagoš, M. Formánek, J. Burša

Faculty of Mechanical Engineering, Brno University of Technology, Technická 2896/2, 616 69 Brno, Czech Republic

1. Introduction

The heart provides pulsatile flow through arteries. In the cardiovascular system, arteries convey nutrient-rich and oxygenated blood to the tissues. Large arteries with a diameter reaching 25 mm gradually taper towards the periphery and branch into smaller arteries. Arterioles with a diameter less than 1 mm are followed by even smaller vessels, capillaries, where the exchange between the blood and tissue cells occurs. The focus of this study is on the arterial periphery and thus on the small arteries. It has been shown that their branching follows a certain order. They form a self-similar asymmetric structured tree, which can be described mathematically [2]. The parent vessel r_p, representing small artery, branches into two smaller arteries (r_{d_1}, r_{d_2}) with radii reduced by coefficients α and β, i.e.,

$$r_{d_1} = \alpha r_p \quad \text{and} \quad r_{d_2} = \beta r_p. \tag{1}$$

The branching is terminated with a minimum radius r_{min} corresponding to the radius of arterioles. The termination has its physiological meaning since the arterioles have approximately the same diameter to ensure even blood supply to organs. Minimum radius r_{min} is constant inside the tree but can vary with different structured trees representing individual organs [2].

The purpose of this work is to assemble a similar system *in vitro*. So far, previous phantom studies have incorporated only pure resistance or two-element Windkessel (2-WK) as an *in vitro* periphery [1], mostly represented by a needle valve and a compliance chamber. Thus, neglecting some of the characteristic features of the arterial periphery, e.g., fluctuations on the input impedance modulus and phase resulting from wave propagation and its reflections within the entire tree with most pronounced reflections at the capillary level. These shortcomings justify the rather smooth waveforms without higher frequency oscillations in phantom experimental measurements, for instance in [1]. Moreover, phase and modulus deviates from reality in both lower and higher frequencies for 2-WK, due to the absence of inertance and characteristic impedance of the root vessel respectively [3, 4]. Including the asymmetric structured tree model in *in vitro* studies as a boundary condition could improve the wave shapes and consequently the overall flow field behaviour (e.g., in an aortic or a carotid phantom).

2. Mathematical model

The wave propagation velocity in small arteries (considered as cylindrical) is much larger than the velocity of the blood flow dominated by viscous forces, leading to the analytical solution of axisymmetric Navier-Stokes equation in the form of pressure $P(x, \omega)$ and flow $Q(x, \omega)$ wave equations. In terms of electrical analogy, the vascular impedance $Z(x, \omega)$ is defined as a ratio

between these wave equations

$$Z(x,\omega) = \frac{P(x,\omega)}{Q(x,\omega)} = \frac{\frac{i}{cC}\left(C_2\cos(\frac{\omega x}{c}) - C_1\sin(\frac{\omega x}{c})\right)}{C_1\cos(\frac{\omega x}{c}) + C_2\sin(\frac{\omega x}{c})}. \tag{2}$$

Eq. (3) based on Eqs. (2) and (4) (from Poiseuille's equation) are the final equations used in the mathematical model [2]

$$Z(0,\omega) = \frac{\frac{i}{cC}\sin(\frac{\omega L}{c}) + Z(L,\omega)\cos(\frac{\omega L}{c})}{\cos(\frac{\omega L}{c}) + icCZ(L,\omega)\sin(\frac{\omega L}{c})} \quad \text{for} \quad x = 0,\ \omega \neq 0, \tag{3}$$

$$Z(0,0) = \lim_{\omega\to 0} Z(0,\omega) = \frac{8\mu l_{rr}}{\pi r^3} + Z(L,0) \quad \text{for} \quad x = 0,\ \omega = 0, \tag{4}$$

where Z is the impedance [kg.m^{-4}.s^{-1}], c is the wave propagation velocity [m.s^{-1}], $C = \frac{3Ar}{2Eh}$ is the compliance [m^2.Pa^{-1}], A is the cross-sectional area [m^2], h is the thickness [m], E is the Young's modulus [Pa], ω is the angular frequency [rad.s^{-1}], x is the axial coordinate [m], $C_{1,2}$ are the constants from general solution of differential equation [–], L is the length of the vessel [m], μ is the dynamic viscosity [Pa.s], l_{rr} is the length to radius ratio [–], and r is the internal radius [m]. The 1D mathematical model of a structured tree is closed with two boundary conditions. A bifurcation condition and a terminal boundary condition, which is determined by zero impedance or constant resistance

$$\frac{1}{Z_p} = \frac{1}{Z_{d_1}} + \frac{1}{Z_{d_2}} \quad \text{and} \quad Z(L,0) = 0,\ Z(L,\omega) = 0. \tag{5}$$

Indexes in this equation correlate with Eq. (1) [2].

The input impedance of the root vessel in the arterial tree includes the resistance of smaller arteries (zero frequency), total arterial compliance (lower frequencies), the characteristic impedance of the root vessel (higher frequencies), wave propagation, and the reflections in the system [4]. The purpose of this model is to describe the input impedance of the structured tree, i.e., the input impedance at the beginning of the root vessel. Since only the impedance at the termination r_{min} is known, the recursive algorithm is necessary to acquire the input impedance [2]. The results can be then validated against experimental measurements *in vitro*.

3. Experimental circuit

For validation of the mathematical model and other experimental measurements, the experimental circuit was assembled (see Fig. 1). The working fluid is moved from reservoir 1 by two-roller peristaltic pump 2, which generates the physiological waveform with specific rotational velocity profile per revolution (found iteratively). The pump is driven by a stepper motor controlled from the MATLAB/Simulink environment, with the usage of Simulink Desktop Real-Time's kernel and Humusoft's I/O device MF634. The circuit also comprises ultrasonic flow meter 3 and two relative pressure sensors 4 and 5 with a sampling frequency of 200 Hz (sufficient to capture the transient pressure waveform). The distance between the pressure sensors was set to 0.6 m, so the pressure loss Δp would be significant and thus measurable for every time step. The transient Δp profile was used to calculate (by pressure-time method) the instantaneous flow rate since the ultrasonic flowmeter provides only the mean flow rate. The evaluation units 6 and 7 serve for individual data collection. The root of the structured tree 8 is connected downstream to the rigid tube with the pressure sensors. The fluid exits the structured tree to the atmospheric pressure and back to reservoir 1. Because the *in vitro* tree is larger in size and less compliant, a slightly higher viscosity of working fluid (mixture of glycerin and water) was chosen in comparison with the real blood to ensure similarity with the *in vivo* impedance, i.e., constant

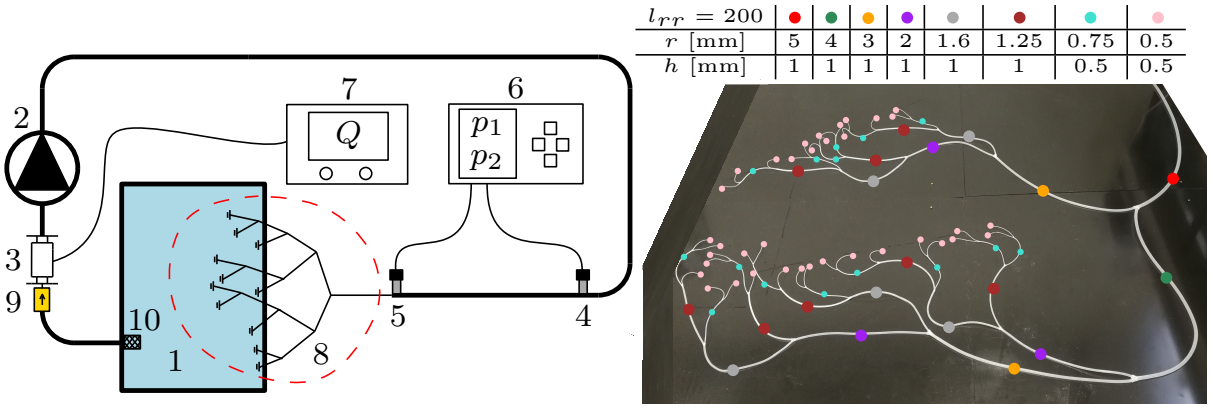

Fig. 1. The scheme of the experimental station for *in vitro* input impedance measurements: 1 – reservoir, 2 – peristaltic pump, 3 – ultrasonic flowmeter, 4 and 5 – pressure sensors, 6 and 7 – evaluation units of pressure and flow, 8 – structured tree (in detail on the right), 9 – non-return valve, 10 – suction filter

viscosity $\mu = 6$ mPa.s and density $\rho = 1126.8$ kg.m^{-3}.

The structured tree consists of small silicon tubes (60 Shore A), which are glued together to form the peripheral vascular site, in detail Fig. 1 (right). It was assumed that the deformations are very small since the maximal pressure in the tube is relatively low, 45 kPa. Therefore, only a few percentages (up to 10%) were included in the determination of E, corresponding to 4.8 MPa. The tube lengths and radii are scaled towards the periphery in a similar manner as can be found *in vivo*, see Eq. (1). To obtain a similar input impedance *in vivo*, the dimensions of the real model had to be scaled according to the limited dimensions and material properties of the commonly available silicon tubes (e.g., internal radii r, thickness h, and Young's modulus E).

The obtained variables from the evaluation units (i.e., the pressure waveform from sensor 5 and flow waveform) need to be transferred from the time-discrete domain to the discrete frequency domain. Doing so, the electrical analogy can be used once again as a simple ratio between the pressure and flow rate. Hence, the frequency-dependent input impedance of the arterial tree is evaluated and can be compared with the mathematical one.

4. Results and discussion

Analytical equations together with the recursive algorithm based on [2] were implemented into MATLAB R2020a. The analytical input impedance is a direct output of the algorithm (blue curve in Fig. 2). The measured waveforms (period $T = 1$ s) were decomposed into cosine waves with corresponding amplitude and phase using the Fourier series. Therefore, the *in vitro* input impedance modulus and phase could be obtained (red curve). Ten harmonics ($n = 10$) were sufficient to describe both waves. The higher the harmonics the smaller is the contained information in signals, which are subjected to noise. Resulting in significantly scattered values of input impedance modulus and phase in higher frequencies. It was mitigated by averaging the input impedance from analyzing multiple periods [4]. For further observation, the human brachiocephalic artery input impedance measured *in vivo* (green curve) [2] is also depicted.

The *in vitro* modulus $|Z_i|$ corresponds very well with the mathematical one, both qualitatively and quantitatively, Fig. 2 (left). Especially in lower frequencies, where the scatter is less pronounced. However, the r_{min} in the mathematical model had to be lowered by 20 %, because of the spread of the gluing into the smallest tubes in the *in vitro* model and thus reducing the internal radius, which led to a higher resistance. The deviation in higher frequencies can be caused by the averaging of multiple periods. Compared to *in vivo* curve, these modules are

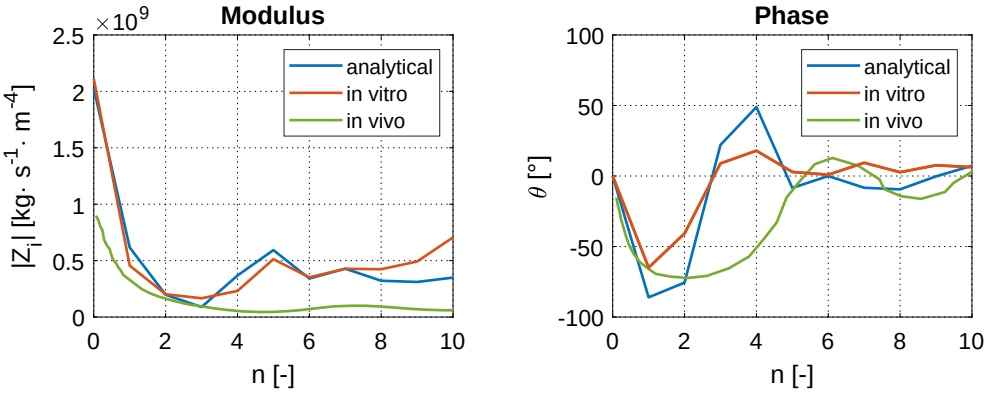

Fig. 2. Comparison of the input impedance modulus $|Z_i|$ and phase θ between *in vitro* experimental measurements (red) and analytical solution from mathematical model (blue), the green curve represents the *in vivo* input impedance of brachiocephalic artery [2], n stands for the number of the harmonics

significantly shifted to higher impedances. Mainly due to the differences in material properties between the arterial wall and 60 Shore A silicon, but also in viscosity and the individual tree geometries (l_{rr}, r_{min}, r, h, α and β).

The right graph represents the phase difference θ between pressure and flow wave for each harmonic. All curves exhibit similar behaviour. Under the lower frequencies, as the total compliance contributes, the phase is negative, i.e., the flow is leading pressure. With increasing frequency the phase becomes positive and then it oscillates to zero values. As the arteries in *in vivo* tree have smaller l_{rr} (around 50), the negative phase is more extensive (green curve).

There are also some facts that could not be described by the mathematical model. Such as a significant decrease in the bifurcation compliance due to the glued bonding between each tube and stepwise diameter reduction between the connected tubes. It may be a source of acceleration in wave propagation causing earlier and unwanted reflections, leading to phase and modulus discrepancies.

Despite all the mentioned limitations and inaccuracies, the overall behaviour of the *in vitro* input impedance is relatively close to the mathematical one. It would be worth improving the real model of the structured tree since the Young's modulus is still very high in comparison with the arterial one. Also, the glued bifurcations and connections between each tube should be eliminated. For example, casting the whole structured tree using the 3D printed moulds would be one option. Another method could be a 3D print of the lumen from wax and then immersion of the luminal model into the pre-mixed silicon with required Young's modulus. After heating the model, the wax would be blown out. Consequently, the *in vitro* and analytical curve would correspond considerably more to the *in vivo* one. Nevertheless, finding a reasonable agreement between the 1D mathematical model and *in vitro* experimental measurements provides an opportunity to design individual structured tree models representing different peripheral sites.

References

[1] Jebbink, E. G., Mathai, V., Boersen, J. T., et al., Hemodynamic comparison of stent configurations used for aortoiliac occlusive disease, Journal of Vascular Surgery 66 (2017) 251-260.

[2] Olufsen, M. S., Peskin, C. S., Kim, W. Y., Pedersen, E. M., Nadim, A., Larsen, J., Numerical simulation and experimental validation of blood flow in arteries with structured-tree outflow conditions, Annals of Biomedical Engineering 28 (2000) 1281-1299.

[3] Vlachopoulos, C., O'Rourke, M., et al., McDonald's blood flow in arteries, CRC Press, 2011.

[4] Westerhof, N., Stergiopulos, N., Noble, M. I., Snapshots of hemodynamics, Springer, 2010.